Investigation on Fatigue Test of Tubing String in High Yield Gas Well

Bo Ning, Ziqiang Liu, Qiuying Li, Yang Ran, Xinyu Kang, Xiaoqiang Guo*

School of Mechatronic Engineering, Southwest Petroleum University, Chengdu, 610500, China

Abstract

Aiming at the problem of corrosion fatigue crack propagation of tubing string in high-yield gas well, the standard compact tensile specimen is prepared with 13Cr-L80 field tubing material, and pre-corroded with field composite phosphate completion fluid. Using MTS electro-hydraulic servo tension torsion fatigue machine, the fatigue corrosion crack propagation test of high-strength 13Cr-L80 tubing material is carried out, and the effects of stress ratio and completion fluid density on the crack propagation life of the tubing string are investigated. The surface of crack propagation zone is analyzed by environmental scanning electron microscope and X-ray energy spectrometer. The results obtained demonstrate that, with the external load stress ratio increasing, the fatigue crack growth rate of the tubing increases, but the range of stress intensity factor decreases, resulting in the intensive of fatigue life. In low-density completion fluid, the crack propagation rate of the tubing string slows down and the fatigue life extends. High-density completion fluid will accelerate the crack propagation rate. Therefore, controlling the stress ratio of the tubing in the range of 0.2~0.25, proper heat treatment or shot peening strengthening of the tubing string and properly reducing the completion fluid density (controlled between 1100 kg/m^3 ~ 1300 kg/m^3) can effectively improve the fatigue life of the tubing string in high-yield gas wells.

Keywords

High-yield Gas Wells; 13Cr-L80 Tubing String; Crack Propagation Test; Crack Growth Rate; Fatigue Life.

1. Introduction

The tubing string of 13Cr-L80 material is widely used in oil fields because of its high strength and good corrosion resistance. During the completion operation of high-yield gas wells, the completion fluid will be used to balance the formation pressure, reduce the damage to the reservoir and maintain the stability of various properties in the gas wells. In order to meet the above demand, compound phosphate completion fluid with high density and protective performance is usually used on-site [1]. During production, the tubing string will be in the corrosive environment of composite phosphate completion fluid, at the same time, the tubing string in service also bears the effects of internal and external pressure, bending deformation, torsional deformation and various loads in the annulus. Under the coupling effect of corrosive environment and alternating load, the tubing string will initiate cracks and expand on the surface, resulting in fatigue failure and causing significant economic losses [2,3].

Some scholars have carried out corresponding research on the corrosion fatigue of tubing string, and achieved some results. Previous scholars have carried out preliminary research on the corrosion fatigue crack prediction model of materials [4-11], and found that the corrosion fatigue is affected by many factors. In recent research, Yang studied and analyzed the stress corrosion cracking performance of X70 steel pipe in simulated deep-sea environment. The results show that the threshold stress of stress corrosion decreases with the increase of hydrostatic pressure and further decreases with the decrease of pH value [12]. Xin carries out fatigue crack growth test on CT specimens prepared from S355 steel and S690 steel. Combined with calculation analysis and numerical simulation, it is found that the greater the stress ratio, the greater the fatigue life, and also affect the threshold value of crack propagation [13]. Luo found that the fatigue crack of the sample made of S135 drill pipe steel initiates from or near the surface of the sample in air. The crack initiation zone in air is cleavage fracture, and the crack propagation zone is fatigue striation. In the marine environment, there are fewer fatigue stripes under high stress amplitude, and the fatigue life is lower than that in air. Fatigue cracks are generated by corrosion pits on and near the sample surface [14]. Considering the influence of loading frequency, Komoda studied the effect of CO containing impurity H2 on hydrogenation accelerated fatigue crack propagation of A333 steel pipe. The addition of CO inhibited the acceleration effect of H2 on fatigue crack growth, and the inhibition effect was affected by the content of CO in H_2, loading frequency and crack propagation rate. The results show that the inhibition effect of CO depends on the competition between the rate of crack propagation to produce a new surface and the rate of CO covering the surface, as well as the time of hydrogen diffusion to the crack tip in the material (CO reduces hydrogen entry) [15]. Wang found that longitudinal cracks or splits often occur in the joint box of drill pipe and drilling tool. The corrosion fatigue of drill pipe and joint is related to hydrogen sulfide and sulfur ions, which may come from the degradation of thread grease or drilling fluid. The statistical analysis results show that the hardness of the material is related to the longitudinal crack of the drill pipe and drill tool joint. The experimental results show that if the hardness of the material is limited below HB310, the longitudinal crack will not expand [16].

In order to effectively solve the corrosion fatigue failure problem of high-yield gas wells and improve the service life of field tubing, this paper carried out an experimental study on the fatigue corrosion crack propagation of high-strength 13Cr-L80 tubing material, and explored the effects of stress ratio and completion fluid density on the corrosion fatigue characteristics of 13Cr-L80 tubing string under the completion fluid corrosion environment, the crack propagation mechanism of the tubing string is revealed.

2. Corrosion-crack Propagation Fatigue Experiment Scheme

2.1. Test Specimen and Equipment

In order to better simulate the field conditions, the 13Cr-L80 tubing material of high-yield gas wells in the west of the South China Sea is processed into a standard compact tensile specimen (CT). The fatigue load direction is the opening direction, and the crack propagation test is carried out. According to GB/T 6398-2017 metal material fatigue test fatigue crack propagation method and equipment fixture requirements, the shape of CT specimen is designed to be 50mm × 48mm×10mm cuboid shape. The geometric size, shape and loading method of the specimen are shown in Fig. 1. The chemical composition and mechanical properties of the tubing materials are shown in Table 1. In order to make the corrosion effect more in line with the site environment, the annulus completion fluid used on site is used as the pre corrosion medium. The formula composition of the completion fluid is shown in Table 1. The test equipment adopts the electro-hydraulic servo tension torsion fatigue machine produced by American MTS system company. The maximum loading load is 250 kN, the vibration frequency is 0.01 Hz ~ 15 Hz, and the maximum stroke is 150 mm, which can meet the index requirements of this crack propagation test. Before the test, the through crack with length of 2.0 mm shall be prefabricated at the gap of CT specimen, and the prefabricated crack shall be completed by sinusoidal tensile load with equal amplitude of 11 kN, stress ratio of 0.1 and loading frequency of 10 Hz. After the test, Quanta 450FEG environmental scanning electron microscope manufactured by American

ISSN: 1813-4890

FEI company was used for surface morphology analysis (SEM) of crack propagation zone and X-ray energy spectrometer for surface element composition analysis (EDS) after corrosion.

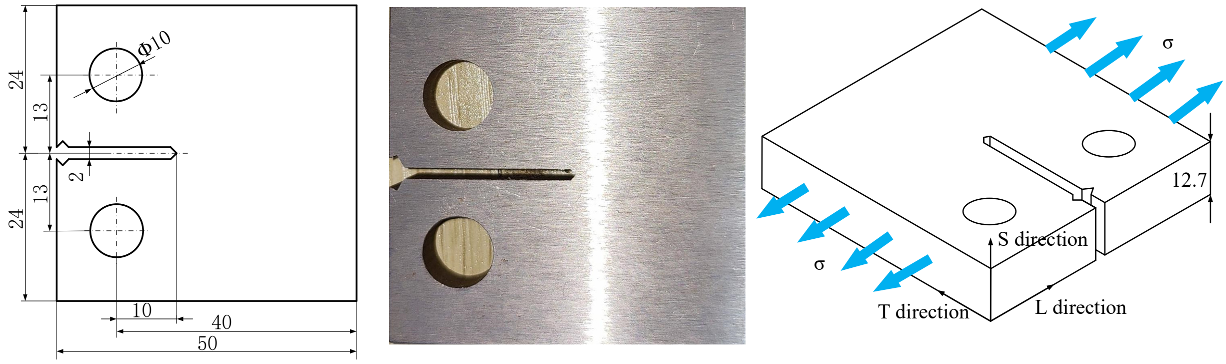

Fig 1. Geometric dimension, shape and loading method of CT specimen

Table 1. Chemical composition and mechanical properties of test materials

Material	Chemical composition (wt%)										Mechanical property		
Tubing (13Cr-L80)	C	Si	Mn	P	S	Cr	Mo	Ni	Ti	Als	Yield limit /MPa	Hardness /HV	Tensile strength /MPa
	0.22	0.48	0.53	0.02	0.001	12.88	2.17	0.04	0.05	0.02	599.6	263.1	771.15
Completion fluid (Pyrophosphoric acid)	Distilled water +0.2%NaOH+0.3%PF-OSY+3%JLB Corrosion inhibitor+$K_4P_2O_7$(Weighted to 1400 kg / m^3)												

2.2. Experimental Principle

(1) Determination of experimental parameters

There are many factors affecting corrosion fatigue, such as stress ratio, load, loading frequency, corrosion medium, load type and applied voltage. When the temperature is constant, the stress ratio, loading load and loading frequency have the greatest influence. Different combinations of stress ratio, loading load and loading frequency will change the failure type of tubing corrosion fatigue. The stress ratio, load and loading frequency range can be obtained from the vibration analysis of high-yield gas well tubing string established by the author [17]. Through calculation, the vibration frequency of high-yield gas well tubing varies from 0.6 Hz to 1.8 Hz, the load varies from 10 kN to 14 kN, and the stress ratio varies from 0.05 to 0.25. In addition, the external corrosive environment will make the amplitude threshold of stress intensity factor smaller than that in simple fatigue, and can also change the crack propagation rate. Therefore, the completion fluid density is also an important factor affecting corrosion fatigue, which can be determined according to the requirements of field operation conditions, with a range of 1000 kg/m^3 ~ 1400 kg/m^3. Consequently, in order to explore the influence of external factors on the fatigue crack propagation characteristics of the tubing and determine the above four factors, five parameter combinations are designed for simulation experiments, as shown in Table 2.

Table 2. Distribution table of crack propagation test parameters

Factor	Test parameters				
Stress ratio	0.05	0.10	0.15	0.20	0.25
Load (kN)	10	11	12	13	14
Loading frequency (Hz)	0.6	0.9	1.2	1.5	1.8
Completion fluid density (kg/m^3)	1000	1100	1200	1300	1400

(2) Experimental steps

In order to simulate the corrosion environment outside the tubing, the composite phosphate completion fluid is used to pre corrode the specimen [18]. The specific operation is to immerse the area to be expanded in the composite phosphate completion fluid for 12 h, as shown in Fig 2(a) below. According to the standard GB 6398-2017 test method, the pre corroded specimen is installed on the electro-hydraulic servo tension torsion fatigue machine, and the COD gauge extensometer (which can detect the output crack length, stress intensity factor and other parameters in real time) is installed. After the pre crack parameters are determined, the pre crack of CT specimen is carried out [19-22]. Based on the pre cracked specimens, determine each group of fatigue crack growth test parameters and carry out fatigue crack growth test (Fig. 2(b)). In this test, the test is completed when the fatigue crack length reaches 35 mm or the crack growth rate exceeds 0.01 mm/cycle. After the fatigue crack growth test, the surface morphology is analyzed by environmental scanning electron microscope and the element composition is analyzed by X-ray energy spectrometer.

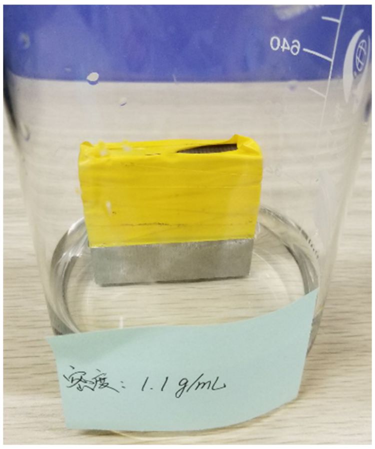

(a) Pre corroded CT specimen

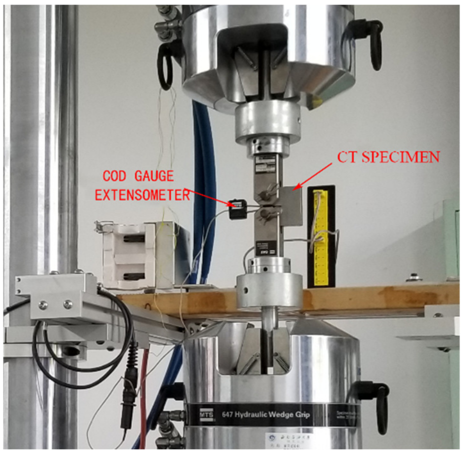

(b) Fatigue crack growth test

Fig 2. Fatigue test treatment

2.3. Treatment of Test Results

The effects of four factors on corrosion fatigue of tubing materials are controlled respectively, and 18 groups of crack propagation tests with different parameter combinations are designed, as shown in Table 3. Fig. 3 is a photo of the crack propagation section of the specimen, in which there are three obviously different areas, including prefabricated crack area, crack propagation area and plastic fracture area. The plastic fracture area is generated by directly breaking the specimen reaching the target crack length by using an electro-hydraulic servo tension torsion fatigue machine in order to better observe the surface morphology of the section. The surface morphology of crack growth zone was analyzed by electron microscope to explore the fatigue crack growth mechanism under different factors.

Table 3. Parameter distribution table of crack propagation test

Serial number	Influence factor				Experimental result	Serial number	Influence factor				Experimental result
	Stress ratio	Loading frequency (Hz)	Load (kN)	Completion fluid density (kg/m^3)	Number of cycles		Stress ratio	Loading frequency (Hz)	Load (kN)	Completion fluid density (kg/m3)	Number of cycles
1	0.05	2	10	1400	45952	10	0.10	1.8	11	1400	34926
2	0.10	2	10	1400	48920	11	0.10	2.0	11	1400	35728
3	0.15	2	10	1400	54137	12	0.10	2.0	11	1300	35327
4	0.20	2	10	1400	61084	13	0.10	2.0	11	1200	35275
5	0.25	2	10	1400	75289	14	0.10	2.0	11	1100	32294
6	0.10	0.6	11	1400	40185	15	0.10	2.0	11	1000	35275
7	0.10	0.9	11	1400	38425	16	0.10	2.0	12	1400	19582
8	0.10	1.2	11	1400	36084	17	0.10	2.0	13	1400	18328
9	0.10	1.5	11	1400	35728	18	0.10	2.0	14	1400	12619

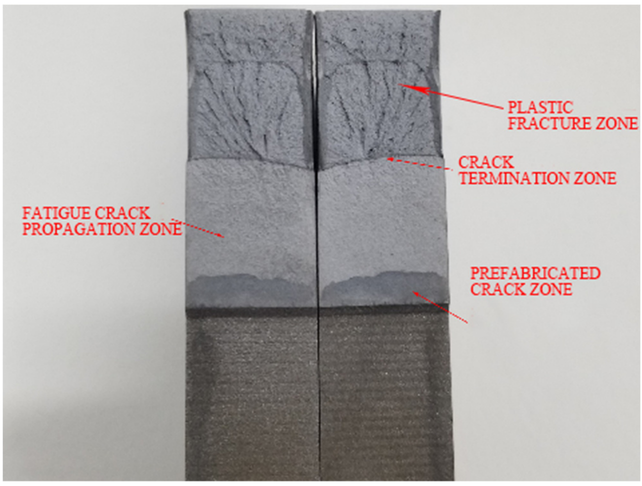

Fig 3. Photographs of fracture surfaces of fatigue specimens

3. Results and Discussion

3.1. Influence of Stress Ratio

Comparing tests 1, 2, 3, 4 and 5, the surface morphology of the crack propagation zone of the specimen under different stress ratios is measured by electron microscope, as shown in Fig 4. Obvious fatigue bands and secondary cracks can be observed in the figure, in which the green frame is the secondary crack. Fatigue bands are groove like samples parallel to each other, which is the most typical microscopic feature of fatigue fracture [23]. Comparing Fig. 4 (a), (b), (c), (d) and (e), it is found that with the increase of stress ratio, the number of secondary cracks on the fracture surface of the sample shows an enhancing trend. According to the basic principle of fracture mechanics [24], the secondary crack can relax the local stress in the plastic

ISSN: 1813-4890

deformation zone at the crack tip, consume the energy of crack propagation, hinder the crack propagation process and improve the fatigue crack life (Fig. 5 (c)).

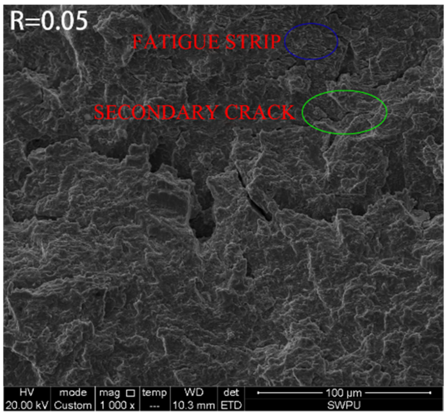

(a) R=0.05

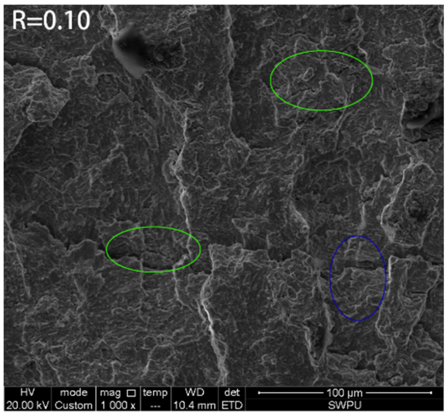

(b) R=0.10

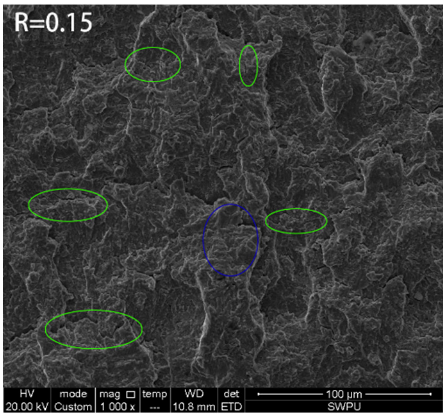

(c) R=0.15

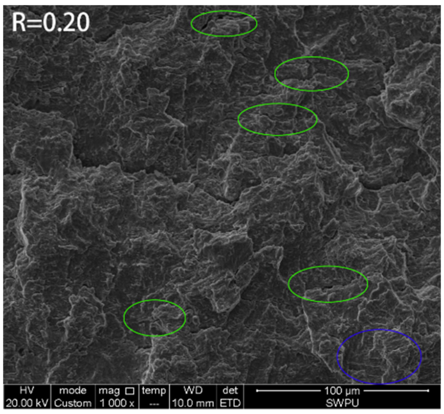

(d) R=0.20

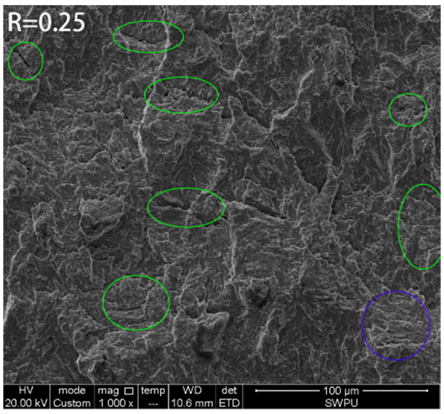

(e) R=0.25

Fig 4. Influence of stress ratio on fatigue crack growth

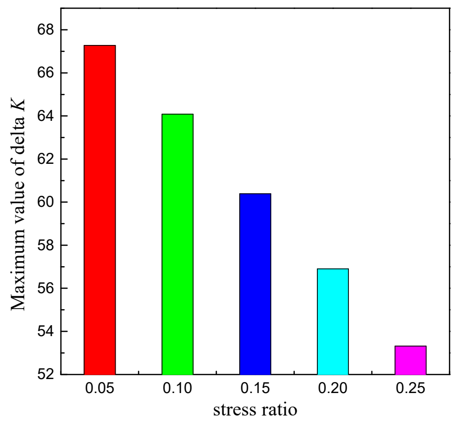

(a) Fatigue crack growth curves under different stress ratios

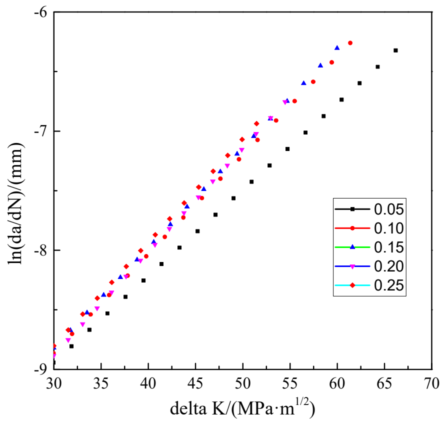

(b) Crack growth curves under different stress ratios

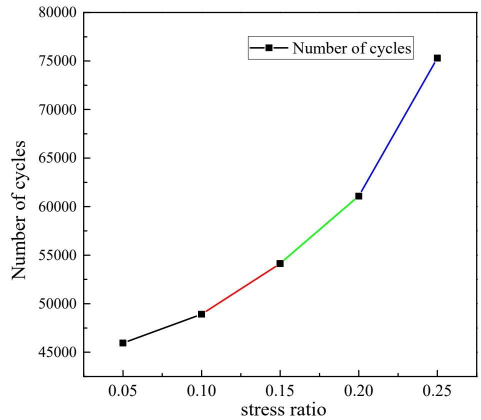

(c) Number of cycles at different stress ratios

Fig 5. Influence of different stress ratios on fatigue crack growth

The test results of stress intensity factor amplitude, crack growth rate and cycle times under different stress ratios are measured by MTS electro-hydraulic servo tension torsion fatigue machine, as shown in Fig. 5. With the enhancement of stress ratio, the range of stress intensity factor amplitude will decrease (Fig. 5 (a)). The main reason is that the larger the stress ratio, the greater the average stress on the specimen, resulting in the decrease of critical stress intensity factor required for material fracture, the augment of the range of stress intensity factor amplitude of 13Cr-L80 pipe and the augment of crack growth rate (Fig. 5 (b)). The main reason is that the stress ratio raises, the proportion of crack opening time increases in the alternating load cycle, and the closing effect decreases accordingly, resulting in the decrease of the threshold value of crack propagation, which improves the crack propagation rate. As shown in Fig. 5 (c), with the enhancement of stress ratio, the number of cycles gradually increases. The main reason for this phenomenon is that high stress ratio will reduce the amplitude range of stress intensity factor. In the crack propagation stage, the stress intensity factor is in a low range. Because there is a positive correlation between the crack propagation rate and the amplitude of stress intensity factor, Therefore, the crack growth rate will also be in a low range, thus increasing the fatigue life.

The influence factors of stress ratio on crack growth rate are mainly the plastic deformation and closure effect at the crack tip. Considering the stress relaxation, according to the G. R Irwin boundary equation of the plastic deformation zone at the crack tip in the plane strain state [25], the average stress field intensity factor km and the boundary equation of the plastic deformation zone at the crack tip can be deduced:

$$\gamma_p = \frac{1}{2\sqrt{2\pi}}\left(\frac{K_m}{\sigma_y}\right)^2 \tag{1}$$

where: γ_p is the boundary dimension of plastic zone; K_I is the stress field intensity factor of mode I crack; σ_y is the yield stress strength. K_m is the average stress field intensity factor, which can be calculated by the following formula:

$$K_m = Y\sigma_m\sqrt{\pi a} = Y\frac{(1+R)}{2}\sigma_{\max}\sqrt{\pi a} \tag{2}$$

where Y is the shape parameter, the deformation work of the plastic deformation zone at the crack tip to be overcome by crack propagation is $\gamma_p \cdot \partial A$, and the plastic deformation zone γ_p at the crack tip is directly proportional to the square of the stress ratio. Therefore, the greater the stress ratio R, the greater the plasticity at the crack tip, and the more energy consumed during crack propagation.

The closure effect is also an important factor affecting crack propagation. Due to the crack closure effect, The driving stress intensity factor of crack propagation is determined by $\Delta K = K_{\max} - K_{\min}$ becomes $\Delta K_{\text{eff}} = K_{\max} - K_{\text{op}}$, Where K_{op} is the minimum stress intensity factor that can make the crack expand when the crack is closed, ΔK_{eff} is the effective stress value of crack propagation during loading. As shown in Fig. 6, in the stress stress intensity factor curve, it can be seen that when the stress intensity factor is within the range of $K_{\min} \sim K_{\text{op}}$, the crack appears closed and cannot expand. When the stress intensity factor is greater than K_{op}, the crack tip can open and expand.

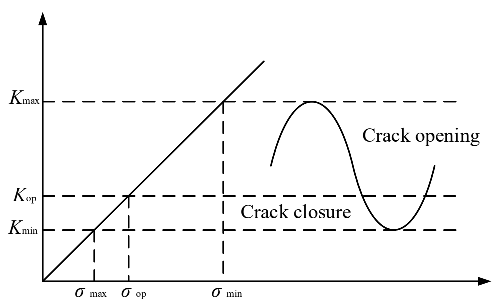

Fig 6. Schematic diagram of crack closure effect

For a specified material, the crack growth opening stress intensity factor is a constant value, when it is determined, there are:

$$K_{\min} = \Delta K \cdot \frac{R}{1-R} \tag{3}$$

It can be seen that $K_{\min}$ increases with the increase of stress ratio R. When the amplitude of stress intensity factor is greater than the threshold value, $K_{\min}\left(R_1\right) < K_{op} < K_{\min}\left(R_2\right)$, where R_1 and R_2 are the stress ratio, and $R_1 < R_2$. At this time, for the stress ratio R_2, the crack can expand in the whole cycle, while for the stress ratio R_1, the crack cannot expand when the stress intensity factor is less than K_{op}. When the crack closure phenomenon occurs, the low stress ratio is more affected by the closure effect, and the crack growth threshold decreases with the increase of the stress ratio. When the stress ratio is greater than the critical stress ratio, the crack growth threshold tends to be stable.

Therefore, during field operation, controlling the external load stress ratio of the tubing in the range of 0.2 ~ 0.25 (Fig. 5 (c)) can effectively improve the fatigue life of the tubing.

3.2. Influence of Completion Fluid Density

According to comparative tests 2, 11, 12, 13 and 14, the corrosion of completion fluid on the specimen material is shown in Fig. 7. The experimental results show that: In clean water, the surface of the specimen is not corroded and no obvious corrosion products are found (Fig. 7(a)). When the completion fluid density is 1100 kg/m^3, the specimen is corroded by the completion fluid and produces a layer of dense corrosion product film attached to the surface of the test piece (Fig. 7(b)), which can effectively slow down the propagation rate in the subsequent crack propagation experiment. In the scanning electric mirror, the material with worse conductivity will show higher brightness, as shown in Fig. 7(c). The highlight in the figure may be a mixture of residual completion fluid and corrosion products. With the further increase of completion fluid density (as shown in Fig. 7(d)), after the completion fluid corrosion, the pits on the surface of the test piece will be filled by corrosion products to alleviate the impact of stress concentration effect caused by pits and reduce the crack growth rate. When the density reaches 1400 kg/m^3 (Fig. 7(e)), its corrosion performance is strengthened and the amount of corrosion products increases. When external load is applied, the corrosion products break and enter the crack, which intensifies the crack initiation, increases the crack propagation rate and reduces the fatigue life.

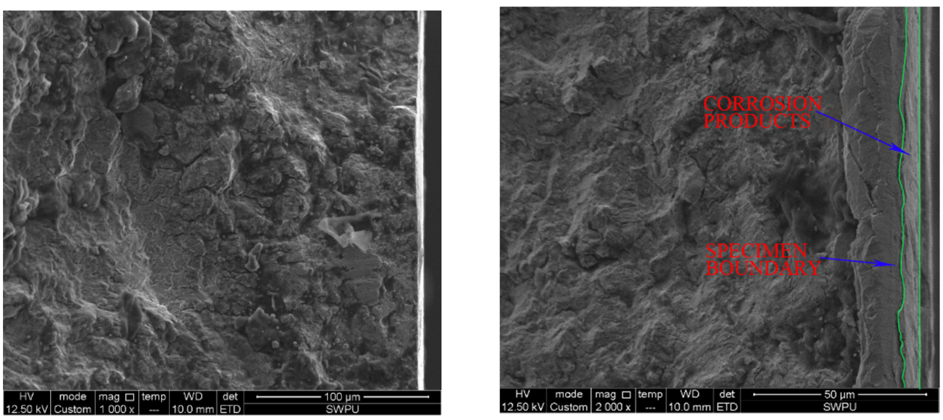

(a) 1000 kg/m^3 (b) 1100 kg/m^3

ISSN: 1813-4890

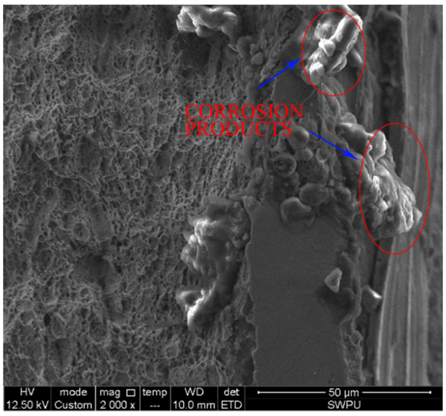

(c) 1200 kg/m^3

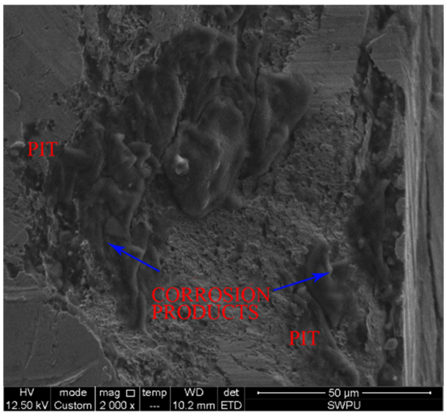

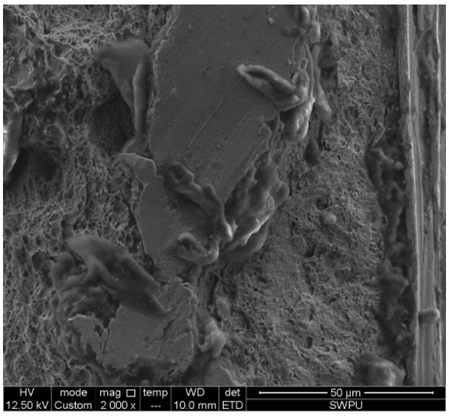

(d) 1300 kg/m^3 (e) 1400 kg/m^3

Fig 7. Surface morphology of specimen section under different completion fluid density

Fig. 8 shows the energy spectrum analysis results of X-ray of tubing specimen after completion fluid corrosion. It can be seen from Fig 8(a) that when there is no corrosion, the surface of 13Cr-L80 tubing is mainly composed of Iron element, followed by Carbon element. The main reason is that the tempered sorbite is formed after carburizing, quenching and tempering treatment, and the surface Carbon content is raised. With the increase of the corrosivity of the completion fluid (Fig. 8(b), (c) and (d)), a chemical reaction occurs on the surface of the tubing, resulting in the dissolution of the surface Iron element into the completion fluid and the increase of the content of Oxygen element. However, because of Carbon element stable chemical properties, it is not easy to have chemical reaction, resulting in enrichment and its content is the largest. At the same time, with the growth of corrosion performance of completion fluid, Iron element is dissolved more seriously and the content is lower and lower. With the increase of Carbon element content, the surface hardness is improved, causing the high-strength 13Cr-L80 tubing is not easy to crack propagation and the fatigue life is improved. When the corrosivity of completion fluid further enhances, the corrosion products on the surface increase, which is easier to break and fall off, promote crack initiation and propagation, improve the crack propagation rate and shorten the fatigue life.

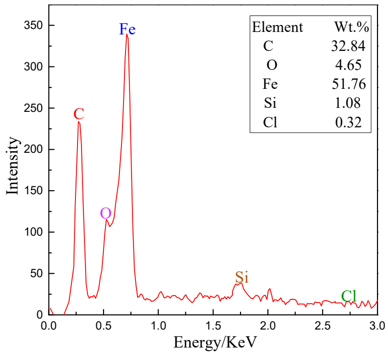

(a) Clean water

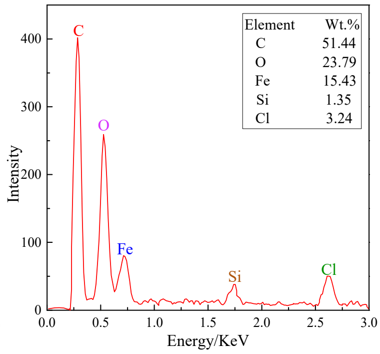

(b) 1100 kg/m³

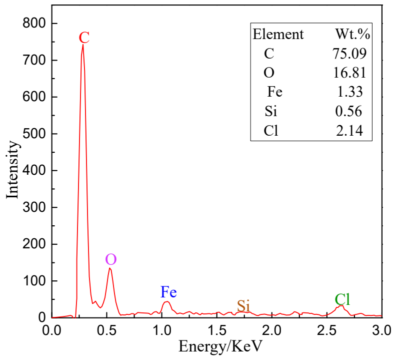

(c) 1200 kg/m³

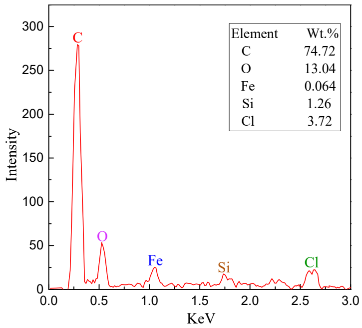

(d) 1300 kg/m³

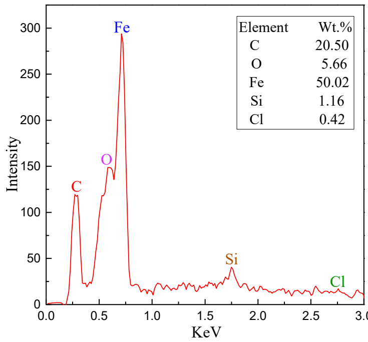

(e) 1400 kg/m³

Fig 8. EDS on specimen surface after corrosion with different completion fluid density

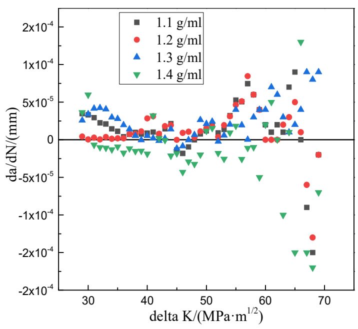

(a) Crack propagation rate after corrosion of completion fluids with different densities

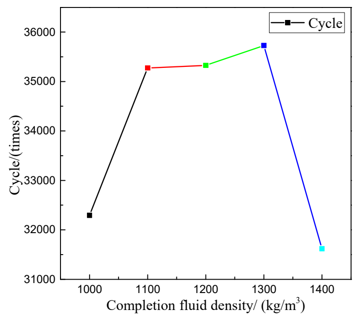

(b) Cycle times after corrosion of completion fluids with different densities

ISSN: 1813-4890

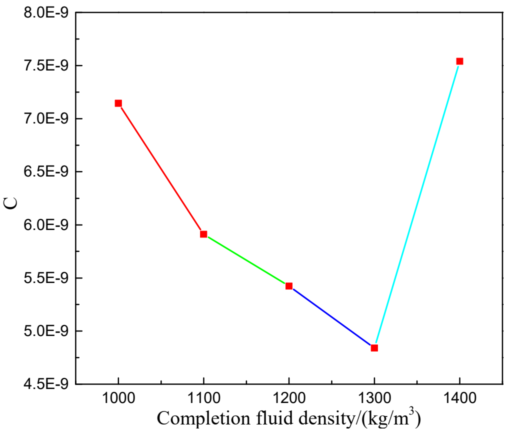

(c) Paris fitting parameter C under different density completion fluid

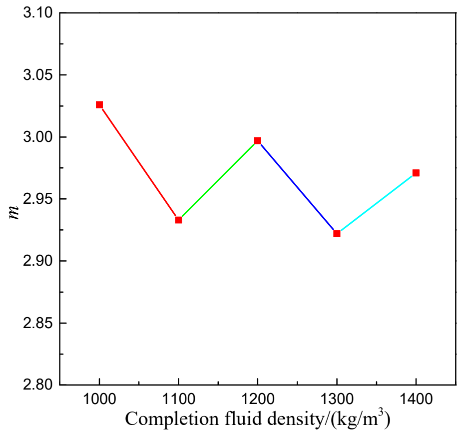

(d) Paris fitting parameter m under completion fluid with different densities

Fig 9. Influence of completion fluid density on crack propagation characteristics of tubing string

The test results of stress intensity factor amplitude, tubing fatigue crack growth rate and cycle times under different completion fluid densities measured by MTS electro-hydraulic servo tension torsion fatigue machine are shown in Fig. 9. Each point in Fig 9(a) shows the difference between the crack growth rate in clean water and that in completion fluid corresponding to the same stress intensity factor amplitude. In Fig 9(a), when the completion fluid density is 1100 kg/m^3, 1200 kg/m^3 and 1300 kg/m^3, the crack propagation rate in completion fluid is slower than that in clean water. The main reason is that with the increase of completion fluid density, The completion fluid will corrode the tubing surface to a certain extent. A layer of corrosion product film is formed on the surface to fill the pits on the tubing surface and prevent the completion fluid from corroding the interior of the tubing. In the crack propagation experiment, the corrosion product film will also reduce the crack propagation rate, increase the content of Carbon element on the surface and enhances the surface hardness, the fracture resistance of tubing is further improved. However, when the completion fluid density exceeds a certain limit, the crack propagation rate of tubing will be accelerated. The main reason is that the completion fluid density is too high, the corrosion products on the surface ars too thick, which is easier to break and fall off, and promote the crack initiation and propagation. In the subsequent crack propagation experiments, it will aggravate the crack propagation rate and eliminate the corrosion products on the surface, The content of Carbon element on the surface decreased, which reduced the fracture resistance of tubing surface. It can be seen from Fig 9(b) that it can effectively show the mitigation and promotion effect of completion fluid density on tubing crack propagation. When the density is 1100 $kg/m^3 \sim 1300$ kg/m^3, the fatigue crack life of tubing will be extended to a certain extent, and when the completion fluid density exceeds 1300 kg/m^3, the fatigue life of tubing will be significantly reduced.

Based on Paris crack propagation model, the amplitude of stress intensity factor and tubing fatigue crack propagation rate under different completion fluid densities are fitted by Paris formula, and the variation curves of material constants C and *m* of crack propagation under different completion fluid densities are obtained. As shown in Fig 9(c), when the density is 1100 $kg/m^3 \sim 1300$ kg/m^3, the Carbon value decreases obviously, and the crack growth rate will slow down, which can effectively improve the fatigue life of tubing. As shown in Fig 9(d), when the density is 1000 $kg/m^3 \sim 1400$ kg/m^3, there is no obvious change in *m* value, indicating that the completion fluid density has little effect on the material constant *m*. Combined with the influence of completion fluid density on material constant, properly reducing completion fluid density can slow down the crack propagation rate.

Therefore, in the process of field operation, on the basis of meeting other conditions, properly diluting the completion fluid density to 1100 kg/m^3 ~ 1300 kg/m^3 can prolong the fatigue life of the tubing.

4. Conclusion

In view of the tubing failure of high-yield gas wells in South China, the CT specimen is prepared with 13Cr-L80 material, and the phosphate completion fluid is used as the corrosion medium to carry out the corrosion fatigue crack growth test. Through the analysis of the results, the following conclusions can be obtained:

(1) In corrosive environment, with the increase of stress ratio, the crack propagation rate increases, but the range of stress intensity factor will be reduced, resulting in the low-speed propagation stage of crack propagation with high stress ratio, which prolongs the fatigue life of the tubing. When the external load is less than the critical load, the crack growth rate decreases with the increase of the external load. When the external load is greater than the critical load, the crack growth rate will increase instantaneously.

(2) The fatigue crack propagation rate of the tubing decreases with the decrease of loading frequency, but the effect of loading frequency on the propagation rate of the 13Cr-L80 tubing is not obvious. The increase of completion fluid density will reduce the crack propagation rate of the tubing. When the completion fluid density is lower than 1300 kg/m^3, the completion fluid will effectively slow down the crack propagation of the tubing. When the completion fluid density exceeds 1300 kg/m^3, the fatigue life of tubing will decrease significantly.

Conflicts of Interest

The authors declare that there are no conflicts of interest regarding the publication of this paper.

References

[1] X.H. Lv, L.L. Liu, J. Li, H.B. Yu, J.F. Xie. Corrosion behavior of titanium alloy in high pH value completion fluid[J]. Rare Metal Materials and Engineering, 2020, 49(07):2326-2332.

[2] J.W. Chen. The research on crack propagation of oil tubing in acidic environment[D].Xi'an Shiyou University, 2017.

[3] [3] W.T. Wang. Research status of corrosion fatigue of metal materials[J]. Light Industry Science And Technology, 2015, 31(02): 33-34+36.

[4] P.C. Paris, Erdogan F.A critical analysis of crack propagation laws[J]. Journal of Basic Engineering, 1963, 85(4):528-533.

[5] R.J. Donahue, H.M. Clark, P. Atanmo, A.J. Mcevily. Crack opening displacement and the rate of fatigue crack growth[J]. International Journal of Fracture Mechanics, 1972, 8(2):209-219.

[6] R.G. Forman, V.E. Kearney, R.M. Engle. Numerical analysis of crack propagation in cyclic-loaded structure[J]. Journal of Fluids Engineering, 1967, 89(3):459-463.

[7] A.J. Mcevily, J. Groeger. On the threshold for fatigue crack growth[J]. Advances in Research on the Strength & Fracture of Materials, 1978:1293-1298.

[8] H.L. Marcus. Environmental Effects(II); Fatigue crack growth in metals and alloys[J]. Lbid, 1978. 365-383.

[9] W.C. Cui. A state-of-the-art review on fatigue life prediction methods for metalstructures[J]. Journal of Marine Science & Technology, 2002, 7(1):43-56.

[10] O. Adedipe, F. Brennan, A. Kolios. Corrosion fatigue load frequency sensitivity analysis[J]. Marine Structures, 2015, 42:115-136.

[11] Y. Huang, X. Ye, B. Hu, L. Chen. Equivalent crack size model for pre-corrosion fatigue lifeprediction of aluminum alloy 7075-T6[J]. International Journal of Fatigue, 2016, 88:217-226.

[12] Z.X. Yang, B. Kan, J.X. Li, Y.J. Su, L.J. Qiao. Hydrostatic pressure effects on stress corrosion cracking of X70 pipeline steel in a simulated deep-sea environment[J]. Journal of Electroanalytical Chemistry, 2018, 822:123-133.

[13] H.H. Xin, José A.F.O. Correia, M. Veljkovic. Three-dimensional fatigue crack propagation simulation using extended finite element methods for steel grades S355 and S690 considering mean stress effects[J]. Engineering Structures, 2021, 227:111414.

[14] S.J. Luo, M. Liu, X.Z. Lin. Corrosion fatigue behavior of S135 high-strength drill pipe steel in a simulated marine environment[J]. Materials and Corrosion, 2019, 70(4):688-697.

[15] R. Komoda, K. Yamada, M. Kubota, P. Ginet, F. Barbier, J. Furtado, L. Prost. The inhibitory effect of carbon monoxide contained in hydrogen gas environment on hydrogen-accelerated fatigue crack growth and its loading frequency dependency[J]. International Journal of Hydrogen Energy, 2019, 44 (54):29007-29016.

[16] P. Wang, X. Wang, L. Han, Y. Feng. Completion fluid induced stress corrosion cracking in HPHT well tubing [J]. Metal Heat Treatment, 2015, 40:191-194.

[17] J. Liu, X. Guo, G. Wang, Q. Liu, D. Fang, L. Huang, L. Mao. Bi-nonlinear vibration model of tubing string in oil&gas well and its experimental verification[J]. Applied Mathematical Modelling, 2020, 81:50-69.

[18] W. Xu. Study on CO2 corrosion of gas field packer under high temperature and high pressure[J]. Journal of Yangtze University(Natural Science Edition), 2015, 12(31):37-40+45.

[19] H. Bian, Q. Zhai, Y. Li, G. Yang, W. Wang, W. Wang. Microstructure and tensile properties of laser deposition repair GH738 superalloy[J]. Chinese Journal of Lasers, 2017, 44(10):73-78.

[20] W. Song. Research on effect of pre-stress on fatigue crack growth behavior of Al-alloy[D]. Chang'an University, 2018.

[21] Z. Zhai, Y. Peng. T. Liu, P. Luan. Effect of stress ratio on fatigue crack propagation threshold value of 25Cr2Ni2MoV steel[J]. Physics Examination and Testing, 2019, 37(01):9-13.

[22] S. Li, S. Li, X. Wang, H. Zhang, Y. Wang, F. Xue. Effect of thermal aging on failure probability of a nuclear primary pipe [J]. Nuclear Power Engineering, 2013, 34(06):138-142.

[23] John W. Fisher,John M. Barsom. Evaluation of Cracking in the Rib-to-Deck Welds of the Bronx–Whitestone Bridge[J]. Journal of Bridge Engineering, 2015, 21(3):138-142.

[24] C.C. Feng. Study on residual stress and fatigue properties of Ti-Ti N-Zr-Zr N multilayer coatings[D]. South China University of Technology, 2015.

[25] J. Cheng, S. Shu. Fracture mechanics[M]. Beijing: Science Press, 2016.